IEEE Access
Multidisciplinary | Rapid Review | Open Access Journal

Received February 6, 2019, accepted March 1, 2019, date of current version April 3, 2019.

Digital Object Identifier 10.1109/ACCESS.2019.2903084

Experimental Testing of Variable Speed Heat Pump Control Strategies for Enhancing Energy Flexibility in Buildings

THIBAULT PÉAN[1,2], RAMON COSTA-CASTELLÓ[2,3], (Senior Member, IEEE), ELENA FUENTES[1], AND JAUME SALOM[1]

[1]Institut de Recerca en Energia de Catalunya, 08930 Sant Adrià de Besòs, Spain
[2]Automatic Control Department (ESAII), Universitat Politècnica de Catalunya, 08028 Barcelona, Spain
[3]Institut de Robòtica i Informàtica Industrial (CSIC-UPC), 08028 Barcelona, Spain

Corresponding author: Thibault Péan (tpean@irec.cat)

This work was supported by the European Union's Horizon 2020 Research and Innovation Programme through the Marie Skłodowska-Curie Grant Innovative controls for renewable source integration into smart energy systems (INCITE) under Agreement 675318.

ABSTRACT Thermal mass of buildings and domestic hot water tanks represent interesting sources of thermal energy storage readily available in the existing building stock. To exploit them to their full potential, advanced control strategies and a coupling to the power grid with heat pump systems represent the most promising combination. In this paper, model predictive control (MPC) strategies are developed and tested in a semi-virtual environment laboratory setup: a real heat pump is operated from within a controlled climate chamber and coupled with loads of a virtual building, i.e., a detailed dynamic building simulation tool. Different MPC strategies are tested in this laboratory setup, with the goals to minimize either the delivered thermal energy to the building, the operational costs of the heat pump, or the CO_2 emissions related to the heat pump use. The results highlight the ability of the MPC controller to perform load-shifting by charging the thermal energy storages at favorable times, and the satisfactory performance of the control strategies is analyzed in terms of different indicators, such as costs, comfort, carbon footprint, and energy flexibility. The practical challenges encountered during the implementation with a real heat pump are also discussed and provide additional valuable insights.

INDEX TERMS Thermal energy storage, demand-side management, heat pumps, model predictive control, building modeling, variable-speed heat pump.

I. INTRODUCTION

The national power grids are confronted to new challenges related to the need for increasing their share of renewable energy sources (RES). To tackle climate change and keep global warming below 1.5°C, the electricity production must be decarbonized deeply and rapidly, among other needed actions in different sectors [1]. Achieving 100% of RES in the grid remains a very challenging goal towards which we must aim. Hydropower already contributes significantly to the penetration of RES in several countries, but this resource is geographically limited to a few sites where it is mostly already exploited [2]. Nowadays, the fastest growing RES consist of solar and wind power: the rapid decline in the cost of these technologies has made them cost-competitive with other fossil or nuclear fuels, and has led to their accelerated deployment [3]. However, the inherent intermittency of these energy sources poses threats to the stability of the grid. To manage high penetration levels of solar and wind power, better ways of matching the supply and the demand will thus be needed [2].

An increased flexibility of the demand-side provides a partial solution to this issue. To achieve a higher degree of load flexibility, storage systems can be implemented and managed as flexible grid assets [4]. In the absence so far of efficient and cost effective batteries or large-scale storage systems, thermal energy storage (TES) represents an interesting alternative to store energy and manage it in a flexible manner [5]. In particular, the present study focuses on two types of TES: water storage tanks and building thermal mass. Water is one of the best storage mediums for low temperature applications, it is widely available and at low cost, therefore

The associate editor coordinating the review of this manuscript and approving it for publication was Hailong Li.

water stratified tanks represent a promising source of TES [6]. Furthermore, small tanks for Domestic Hot Water (DHW) are already installed in a significant share of residential buildings, representing a large storage potential where flexibility can be activated. The air and structural mass of a building can also be exploited for short-term energy storage: they are highlighted as a key technology for implementing demand-side management (DSM) [7] because they are readily available and do not require further equipment investment. Both water tanks and thermal mass show promising potential to enhance the energy flexibility of buildings [8]. Numerous studies have already proven that they can effectively be used with that purpose, for example by means of load-shifting [9], storing excess energy from an on-site RES plant [10], and resulting more cost-effective than batteries [11].

To couple TES with the electrical grid, heat pumps is considered the most efficient solution [12]. Supervisory control for improving demand-side flexibility with heat pumps has largely been investigated in recent literature [13], especially in the form of simple rule-based controls or model predictive control (MPC) schemes. They display great potential for facilitating demand-side management, RES integration [14] and load-shifting [15].

The present study investigates MPC strategies for controlling a heat pump in a residential building and thus enhancing its energy flexibility in both heating and cooling mode. The work was carried out experimentally in a laboratory setup with a real heat pump system, thus providing insights on the actual performance of such strategies. The study intends to address several gaps identified in the existing literature on this topic.

Firstly, few experimental studies provide detailed information on the behavior of a real heat pump operating under a model predictive control framework. Most works published on this topic rely on simulation models [16], [17] that consider the heat pump as a black box that supplies the thermal power required by the predictive controller, in the fashion of an ideal heater or cooler. On the other hand, most of these previous works are based on catalogue data for evaluating the coefficient of performance (COP) of the system. Certain dynamic and transient effects of the heat pump are neglected (e.g. delays, ramping, cycling, stand-by, model mismatch) but these can affect the performance of the controller and should be investigated further, as suggested notably by the review of Fischer and Madani [12]. De Coninck and Helsen [18] reports the application of an MPC in an actual office building based on the comparison of the plan of the controller with the actual operation of the systems, but do not analyze the heat pump operation in detail. Within this context, the present study explores the dynamic behavior of a real heat pump under an MPC scheme, paying particular attention to analyzing the discrepancies between the predicted and actual operation of the system. For this, experiments are carried out in a semi-virtual environment, with a variable-speed heat pump (VSHP) placed in a climate chamber and coupled to a virtual building model. Furthermore, implementing such controller on a real heat pump enables identifying the practical challenges faced during the deployment phase, in particular regarding the method for interfacing the controller with the physical systems, the commands to be sent to control the heat pump and the interaction of the supervisory control with the built-in local controller of the machine. Such information is important regarding the feasibility and large-scale deployment of MPC controllers for heat pumps. Recent efforts were made to facilitate the flexible control of heat pumps such as the ''SG-ready'' label in Germany [19], but further investigations are necessary.

Secondly, most of the literature concerning MPC for building climate control resort to a simple energy savings objective [20], or to economic optimization [13], i.e. the minimization of the operational costs. Monetary savings in the range of 15 to 40% are reported [16]–[18] when time-varying electricity tariffs are applied, sometimes despite an increase of the energy use. However, since the actual goal of energy flexibility consists in limiting the environmental impact of Heating, Ventilation and Air Conditioning (HVAC), momentum is moving towards optimization of the carbon footprint rather than the costs [21]. A few recent studies include in their framework the minimization of the CO_2 emissions derived from the heat pump use [22]–[24]. In particular, the use of the marginal CO_2 emissions is deemed to represent more accurately the carbon footprint of DSM strategies, given that they take into account the merit order of the plants activated in a given power grid [25]. The marginal emissions differ from the average emissions of the grid: they correspond to the emissions of the marginal plants used to absorb variations of the overall load in that grid. For this reason, calculating the emissions savings with the marginal CO_2 signal provides a more accurate representation of the environmental impact of DSM actions.

The present article will thus compare different MPC configurations, aiming to either minimize the thermal energy delivered to the building, the operational costs or the marginal carbon footprint related to the heat pump use. To achieve these objectives, all strategies utilize the thermal storage of the building (envelope and water tank), storing energy at favorable times and discharging it later. They will be analyzed under the same Key Performance Indicators (KPIs) to indicate which configuration is better suited to achieve which goal.

Finally, the MPC developed in the present work is adapted for the reversible heat pump to operate both in heating and cooling mode. To the authors' knowledge, the use of the same heat pump for providing energy flexibility in different seasons has seldom been investigated. Hurtado *et al.* [26] notably compared the flexibility potential in hot or cold climates, but did not consider a temperate climate in which the heating and cooling demands are balanced throughout the year. Lee *et al.* [27] analyzed a reversible heat pump in both heating and cooling mode, but that was only operated with simple rule-based control, therefore the MPC specificities were not discussed (the required modeling in particular).

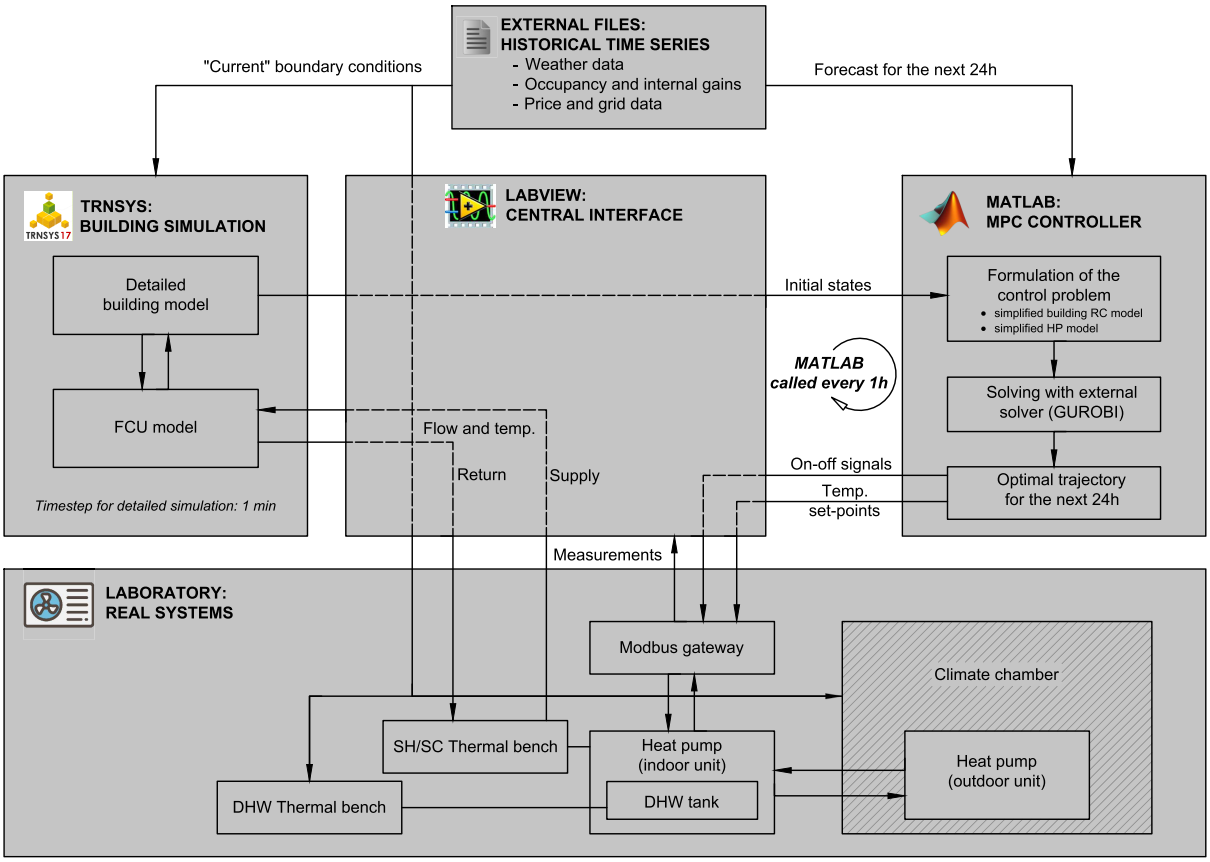

FIGURE 1. Schematic of the co-simulation and the software environment.

For these reasons, the operation of the VSHP with MPC in heating and cooling mode will be discussed here, especially the adaptations needed to switch from one to the other, along with specifications linked to the seasonal operation. For the purpose of analyzing the performance of the system under a climate zone with similar levels of energy demand in winter and summer, the scenario selected for this study is a residential building situated in the Mediterranean area of Spain, where the cooling and heating needs are comparable in magnitude.

To summarize, the novelties brought up by the article compared to existing literature can be summarized by the following points:

- The experimental nature of the work provides more realistic and valuable results than most of the existing simulation work, and the detailed description of the methodology and design of the semi-virtual environment setup enable a further reproducibility of the work;
- Reporting the implementation of MPC control strategies with a real heat pump enables to highlight certain practical bottlenecks;
- The comparison of different MPC objectives for enhancing the energy flexibility of residential buildings demonstrates which configurations perform best;
- Among these, the novel introduction of a CO_2 minimization objective, seldom investigated, proves how well-designed control can be used to limit the carbon footprint of HVAC energy use;
- Applying the same flexibility strategies with a reversible heat pump, for heating in winter and cooling in summer, along with the description of the needed adaptations, demonstrates how the energy flexibility potential can be leveraged in different seasons.

The article firstly presents the methodology, meaning the laboratory setup, the tested heat pump machine and the MPC framework with its algorithms, constraints and models. The results of the experiments are next reported: dynamic tests of three days duration in cooling and heating mode were carried out. Different MPC configurations were tested with the same boundary conditions, so as to be able to analyze their respective performance. The dynamic study cases are analyzed with regards to their energy efficiency, flexibility, comfort, costs and carbon footprint. Finally, discussions and conclusions are drawn, focusing on the aforementioned aspects.

II. METHODS: TEST OF MODEL PREDICTIVE CONTROLS WITH A REAL HEAT PUMP

A. PRINCIPLE OF THE TESTS AND FRAMEWORK OF THE CO-SIMULATION

The performed tests were carried out in a semi-virtual environment. The schematic of the control and communication set up is presented in Fig. 1. The Labview interface centralizes

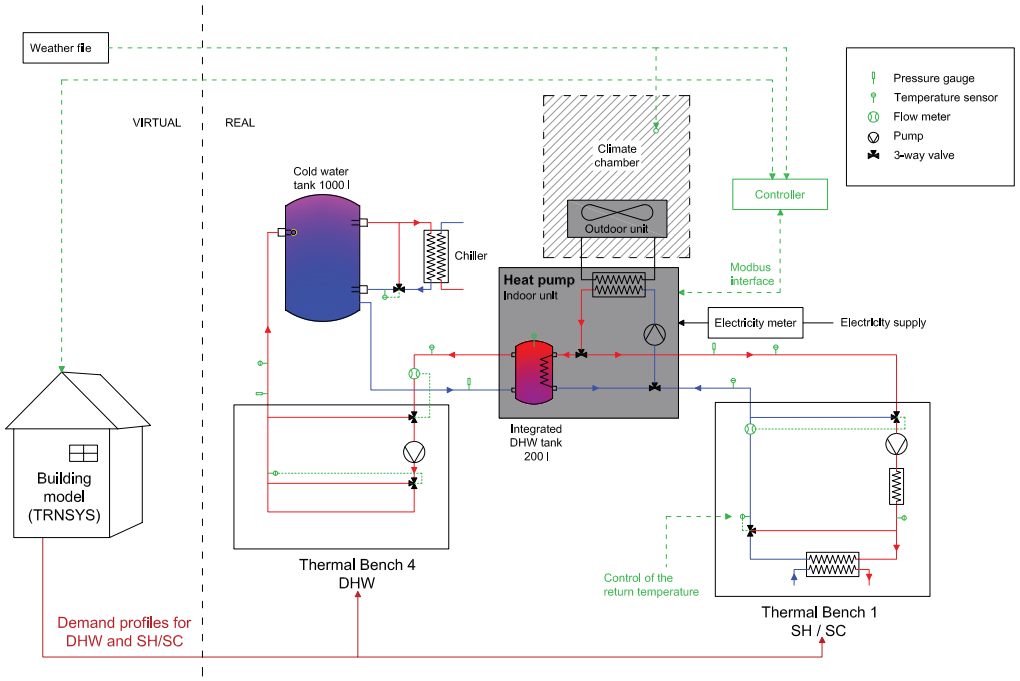

FIGURE 2. Mechanical schematic of the experimental setup.

all the commands and exchange of variables between the different software. The TRNSYS simulation [28], set to a calculation time step of 1 minute, calculates the energy loads of the real building, and thus serves as a virtual plant that enables testing the different control strategies. The MPC controller is implemented externally in MATLAB to benefit from its optimization features, similarly to the method applied in [29]. External files containing time series data of weather, occupancy and grid variables provide the necessary input for TRNSYS. The same weather conditions are emulated dynamically in the laboratory climate chamber in which the heat pump is placed. The DHW tapping profiles are another input to the simulation model and the laboratory testing. Considering perfect predictions, the external files also provide the forecasts necessary for the MPC to project the future behavior of the systems. The acquisition system saves the measured data with a frequency of 10 s, while it updates the control set-points for the laboratory every minute.

B. TESTED HEAT PUMP SYSTEM

The major contribution of the present work consist in testing the adopted control strategies on a real heat pump system, to evaluate their performance in a more realistic setup. A heat pump is a thermodynamic machine that makes use of a closed circuit of refrigerant fluid to transfer heat from one fluid (the source) to another (the sink). An electrically-driven compressor enables running the cycle of compression and decompression of the refrigerant fluid necessary between the two heat exchangers. In the present case, we consider an air-to-water heat pump, therefore the source fluid is the outdoor air and the sink fluid is a water circuit (linked to the building).

The chosen machine is a reversible air-to-water heat pump from the Hitachi Yutaki series. It can work at variable speed like most heat pumps in the market, since the compressor is inverter-driven. Its nominal power is 11 kW in heating mode for a COP of 3.98 and 7.2 kW in cooling mode for an Energy Efficiency Ratio (EER) of 3.3.[1] It consists of a split system: it counts with an outdoor unit with the heat exchanger and fan, and an indoor unit which includes a 200 liters water tank to store DHW and an internal controller.

C. LABORATORY SEMI-VIRTUAL ENVIRONMENT

The experiments are carried out in a semi-virtual environment laboratory setup, of which the mechanical schematic is represented in Fig. 2. The concept of semi-virtual environment consists in coupling a real device (a heat pump in the present case) with a virtual simulation software (building simulation in TRNSYS in the present case). Such setup is used in many laboratories where energy flexibility of buildings is tested [30]. The air-to-water heat pump is installed as shown in Fig. 3: the outdoor unit is placed into a climate chamber, and the floor standing indoor unit containing the DHW tank is placed outside the chamber in the laboratory space room. Both units are connected through a refrigerant fluid circuit. The walk-in climate chamber is a 45 m^3 room space, where the air properties can be controlled in a temperature range of -30 to $+60°C$ and a relative

[1] According to EN14511 [40], standard rating conditions in heating mode: outside air temperature 7°C, inlet water temperature 40°C, outlet water temperature 45°C. In cooling mode: outside air temperature 35°C, inlet water temperature 12°C, outlet water temperature 7°C.

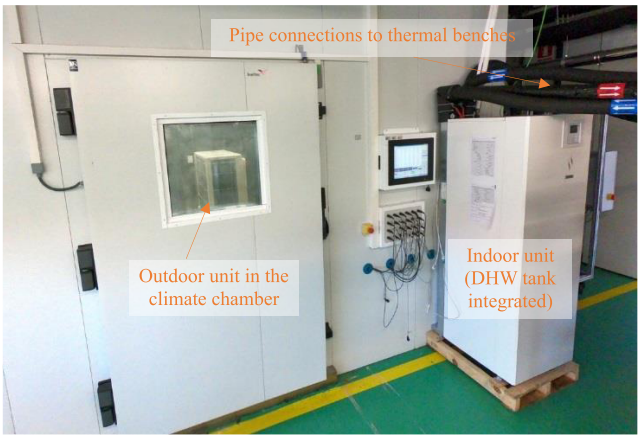

FIGURE 3. Photograph of the laboratory installation (heat pump and climate chamber).

humidity range of 15 to 98%, enabling to recreate a wide spectrum of climatic conditions. In the reported experiments, this climate chamber is used to emulate dynamically the outdoor conditions of the chosen location. Such setup enables to perform repetitive experiments with the exact same boundary conditions and thus to ensure reproducibility and a valid comparison between the different control configurations.

The coupling between the virtual building and the heat pump is done by means of two thermal benches. The first thermal bench emulates the space heating or cooling load from the building Fan Coil Units (FCU): when the heat pump runs in this mode, its output water flow and temperature are recorded. The laboratory measurements of supply temperature and water flow are sent to the TRNSYS building model, which calculates the corresponding return temperature considering the dynamics of the building. This return temperature is emulated with the thermal bench that extracts or delivers heat to the water flow by means of a heat exchanger to reproduce the thermal load of the building.

In all the presented experiments, the water flow in the heat pump circuit is kept at a constant value of 26 l/min for the space heating/cooling loop and 33 l/min in the internal DHW tank charging loop, both in the normal range of operation of the machine.

A second thermal bench allows reproducing the DHW tapping profiles of the building occupants. Following a predefined daily tapping schedule derived from the standard [31], a water flow is drawn from the top of the DHW tank, so as to deliver 45°C at the tapping point. A buffer tank with cold water (1000 liters) is used to provide water at the temperature of the mains network during the DHW extractions. This tank is kept at a temperature of 10°C in the winter cases, and 19°C in the summer cases. The water from the bottom of this cold tank is circulated into the heat pump DHW tank during each tapping event. The water flow during the DHW extractions is controlled with the 3-way valves and a flow controller loop in the corresponding test bench.

D. STEADY-STATE HEAT PUMP EXPERIMENTS AND MODELLING

To characterize the efficiency of the heat pump, steady-state tests were conducted in the laboratory with the thermal bench 1 (as shown on the right side of Fig. 2). The static tests consisted in fixing the triplet of temperatures $(T_{sup}, T_{ret}, T_{amb})$: the supply set-point temperature T_{sup} is set in the local controller of the heat pump, the return water temperature T_{ret} is controlled in the thermal bench of the laboratory, and the ambient temperature T_{amb} is controlled by the climate chamber where the outdoor unit is situated. This way, a broad range of operating conditions was tested. For each static point, the following variables were measured and averaged over 30 minutes in stationary conditions: water supply and return temperatures T_{sup} and T_{ret}, air temperature in the chamber T_{amb}, electrical power draw P_{el}, thermal capacity Q and resulting $COP = Q/P_{el}$. From the performance map obtained with these measurements, a black-box model was derived, in the form of a polynomial regression of the electricity consumption of the heat pump as a function of the operating temperatures. This process was repeated in heating and cooling mode, since the operation of the heat pump is significantly different in these two operation modes. The two equation models obtained are indicated in (1) and (2). However, the equation of P_{el} must remain linear to be used in the MPC, therefore the dependency of T_{sup} on Q must be removed. Instead, different operating points are chosen, representative of the functioning of the heat pump: $T_{sup,SH,0} = 35°$ for space heating, $T_{sup,TES,0} = 55°$ for production of DHW, and $T_{sup,SC,0} = 10°$ for space cooling. The total power draw of the heat pump is modelled with equation (3) and (4), it consists of one term $P_{el,SH/SC}$ for the space heating/cooling mode and one term $P_{el,TES}$ for the DHW production mode (the device switches between modes when operating normally).

$$\begin{aligned} P_{el,SH} &= \left[\frac{1}{COP}(T_{sup}, T_{amb})\right] \cdot Q_{SH} \\ &= \left[a_0 + a_1 T_{sup} + a_2 T_{amb} + a_3 T_{amb}^2 \right. \\ &\quad \left. + a_4 T_{sup} T_{amb}\right] \cdot Q_{SH} \end{aligned} \tag{1}$$

$$P_{el,SC} = c_0 + c_1 T_{amb} + c_2 T_{sup} + c_3 Q_{SC} \tag{2}$$

$$\begin{aligned} P_{el,tot,SH} &= P_{el,SH} + P_{el,TES}. \\ &= \left[\frac{1}{COP}(T_{sup,SH,0}, T_{amb})\right] Q_{SH} \\ &\quad + \left[\frac{1}{COP}(T_{sup,TES,0}, T_{amb})\right] Q_{TES} \end{aligned} \tag{3}$$

$$\begin{aligned} P_{el,tot,SC} &= P_{el,SC} + P_{el,TES} \\ &= \left[c_0 + c_1 T_{amb} + c_2 T_{sup,SC,0} + c_3 Q_{SC}\right] \\ &\quad + \left[\frac{1}{COP}(T_{sup,TES,0}, T_{amb})\right] Q_{TES}. \end{aligned} \tag{4}$$

E. BUILDING STUDY CASE

The present article focuses on residential buildings situated in the Mediterranean area of Spain. Such construction

typologies present interesting characteristics: their heating and cooling loads are notably balanced over the year, which enable benefitting from the flexibility both in summer and winter. Furthermore, residential buildings are the most common typology in Spain and represent the largest share of energy use from buildings, especially regarding their thermal loads [32].

The chosen building study case is a residential flat of 109 m^2 situated in a building block in the Mediterranean climate of Spain and can accommodate a family of four members. A circuit of Fan-Coil Units supplied by the heat pump enables to condition the indoor space. The walls are highly insulated with a U-value of 0.2 W/m^2K.

As shown in Fig. 1, two models of this building are necessary for the experimental setup to function: a detailed building model which acts as a substitute of the real building and runs in real time (time step of 1 minute), and a reduced order model for the MPC controller (discretized with time step of 12 minutes). The detailed model is set up in TRNSYS and allows calculating in a high degree of detail the thermal dynamics occurring in the dwelling. More information on the building model can be retrieved from previous publications [33].

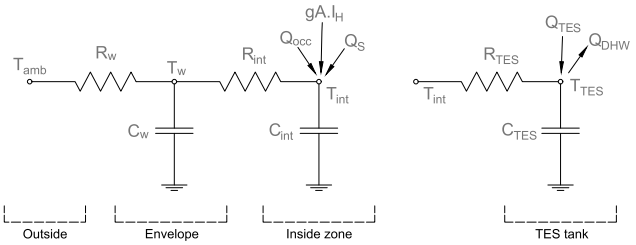

FIGURE 4. Reduced order model of the building envelope and the DHW tank. The arrows represent the heat fluxes at every node.

TABLE 1. Parameters of the RC model for heating and cooling.

Coefficient	Unit	Value (heating)	Value (cooling)
R_{int}	K/kW	1.09	0.29
R_w	K/kW	9.01	9.4
R_{TES}	K/kW	601	601
C_{int}	kWh/K	1.77	1.77
C_w	kWh/K	24.2	45.6
C_{TES}	kWh/K	0.29	0.29
gA	m^2	1.95	1.56

F. BUILDING SIMPLIFIED MODELLING

On the other hand, the simplified model consists of a resistance-capacitance (RC) reduced order model, as shown in Fig. 4. This model contains three temperature states $x = [T_{int} T_w T_{TES}]^T$:

- T_{int} is the mean operative temperature of the indoor zone,
- T_w is an intermediate average temperature at the internal surface of the external walls,
- T_{TES} is the average water temperature of the tank storing DHW in the heat pump.

Two states (T_{int} and T_w) are generally considered sufficient to model the building envelope for this kind of application [34]. The simplified model contains 7 parameters:

- R_{int}, R_w and R_{TES} expressed in K/kW, are the thermal resistances of the inside air node, of the external walls and of the tank insulation respectively.
- C_{int}, C_w and C_{TES} expressed in kWh/K, are the thermal capacitances of the inside air node, of the external walls and of the tank water respectively.
- gA, expressed in m^2 is the aperture area, a coefficient that buffers the solar irradiation entering the building.

The parameters of the building part of the model were obtained through a model identification process using a method similar to the one applied in [35], which is based on grey-box modelling. Data obtained from the detailed TRNSYS model was generated for this purpose, exciting the model with a pseudo-random binary signal on the thermal power delivered to the building. This process enables to cover different ranges of the thermal dynamic behavior of the flat, and thus facilitates the identification procedure. The obtained values are presented in TABLE 1 and they are different for summer and winter: the model identification process was repeated in both seasons, so as to obtain more suitable models in cooling and heating modes respectively.

The obtained values of the capacitances reflect the storage capacity of the building. For the envelope, $C_{int} + C_w$ ranges from 26 to 47 kWh/K, but the range of allowed temperature variations is low (around 2°C) and not all the capacity of the walls can be exploited (only until the insulation for instance). The capacity of the water tank is smaller: $C_{TES} = 0.29\ kWh/K$, but greater temperature variations can be exploited in the tank (up to 10 or 15°C for instance) for storing energy.

The behavior of the model is affected by two types of inputs: controllable inputs $u = [Q_S\ Q_{TES}]^T$ and exogenous non-controllable inputs $e = [T_{amb}\ I_H\ Q_{occ}\ Q_{DHW}]^T$ where:

- Q_S and Q_{TES}, expressed in kW, represent the thermal power delivered by the heat pump to the indoor zone through the FCU and to the TES tank respectively.
- T_{amb} and I_H are the weather conditions: outdoor temperature in °C and solar irradiation in kW/m^2 respectively.
- Q_{occ} and Q_{DHW}, expressed in kW, represent the occupant behavior. These terms represent the heat gains from the presence of occupants in the indoor space, and the hot water tapping which follows a standard tapping profile [31].

To summarize, the simplified building model can be formulated in continuous state-space as in (5), which results from writing the heat transfer equations between the different states of the model. The matrices in continuous form are superscripted with c, and are later discretized with a time step

Problem 1 Model Predictive Controller

Objective:

$$\min_{\upsilon\delta}\left[\alpha_\varepsilon J_\varepsilon + \alpha_{\Delta u} J_{\Delta u} + (1-\alpha_\varepsilon-\alpha_{\Delta u}) J_{obj}\right]$$

Subject to: $\forall k \in [\![1, N]\!]$

Model:

$$\begin{cases} \boldsymbol{x}(k+1) = \boldsymbol{A}\cdot\boldsymbol{x}(k) + \boldsymbol{B_u}\cdot\boldsymbol{u}(k) + \boldsymbol{B_e}\cdot\boldsymbol{e}(k) \\ \boldsymbol{y}(k+1) = \boldsymbol{C}\cdot\boldsymbol{x}(k) \end{cases}$$

Constraints on the inputs:

$$\begin{cases} \delta_S(k)\cdot\underline{Q_S} \le Q_S(k) \le \delta_S(k)\cdot\overline{Q}_S \\ \delta_{TES}(k)\cdot\underline{Q_{TES}} \le Q_{TES}(k) \le \delta_{TES}(k)\cdot\overline{Q}_{TES} \\ \delta_S(k) + \delta_{TES}(k) \le 1 \end{cases}$$

Constraints on the outputs:

$$\begin{cases} \underline{T_{int}}(k) - \varepsilon(k) \le T_{int}(k) & (heating) \\ T_{int}(k) \le \overline{T}_{int}(k) + \varepsilon(k) & (cooling) \\ \underline{T_{TES}} - \varepsilon(k) \le T_{TES}(k) & (\varepsilon \ge 0) \end{cases}$$

of 12 minutes to be used in the MPC framework (matrices A, B_u, B_e and C without superscript). The vector of outputs $y = [T_{int}\, T_{TES}]^T$ is a subset of the vector of states x, discarding the wall temperature T_w.

$$\begin{cases} \boldsymbol{x} = \boldsymbol{A^c}\boldsymbol{x} + \boldsymbol{B_u^c}\boldsymbol{u} + \boldsymbol{B_e^c}\boldsymbol{e} \\ \boldsymbol{y} = \boldsymbol{C^c}\boldsymbol{x}. \end{cases} \tag{5}$$

With:

$$\boldsymbol{A^c} = \begin{bmatrix} -\frac{1}{R_{int}C_{int}} & \frac{1}{R_{int}C_{int}} & 0 \\ \frac{1}{R_{int}C_w} & -\frac{1}{R_wC_w} - \frac{1}{R_{int}C_w} & 0 \\ \frac{1}{R_{TES}C_{TES}} & 0 & -\frac{1}{R_{TES}C_{TES}} \end{bmatrix},$$

$$\boldsymbol{B_u^c} = \begin{bmatrix} \frac{1}{C_{int}} & 0 \\ 0 & 0 \\ 0 & \frac{1}{C_{TES}} \end{bmatrix}, \boldsymbol{B_e^c} = \begin{bmatrix} 0 & \frac{gA}{C_{int}} & \frac{1}{C_{int}} & 0 \\ \frac{1}{R_wC_w} & 0 & 0 & 0 \\ 0 & 0 & 0 & -\frac{1}{C_{TES}} \end{bmatrix}$$

and

$$\boldsymbol{C^c} = \begin{bmatrix} 1 & 0 & 0 \\ 0 & 0 & 1 \end{bmatrix}$$

G. TESTED MPC CONFIGURATIONS

The Optimal Control Problem (OCP) of the MPC algorithm is presented in Problem 1: it intends to generate a control action that minimizes an objective function over a prediction horizon N, taking into account the dynamics of the buildings through a model, and certain constraints set on the inputs and outputs.

The model has already been presented in section II.F.; the multi-objective function is explained in section II.G.1 and the constraints in section II.G.2. For the prediction horizon, a value of 24 hours is chosen, i.e. $N = 120$ time steps, considering a discretization time step of 12 minutes for the model of the MPC. Such value is common practice for building climate control applications, since it enables to take into account the daily variations occurring naturally in weather and occupancy parameters [36].

1) OBJECTIVES

The proposed MPC framework consists in a multi-objective minimization: the cost function comprises three objectives J_ε, $J_{\Delta u}$ and J_{obj}. $J_{\Delta u}$ is a smoothing term which penalizes too many consecutive changes in the control actions, as shown in (6). J_ε is a comfort objective, it actually intends to minimize discomfort by avoiding violations of the imposed comfort range. The hard constraints on the outputs are softened by the slack variable ε which is included in this objective term, as seen in (7) (see also section II.G.2) for more details on the constraints softening).The actual flexibility objective is denominated J_{obj}, and it can take three different forms: minimization of the thermal energy delivered to the building J_{en}, of the operational electricity costs J_{cost}, or of the CO_2 marginal emissions related to the heat pump use J_{CO2}. These three different formulations are presented in (8) to (10). In (8), the efficiency of the heat pump is not taken into account, only the final thermal energy delivered to the inside zone. In (9) and (10), the objective functions take into account the varying performance of the heat pump through the electricity use $P_{el,tot}$ taken from (3). This electricity use is then multiplied by a normalized penalty signal: E_{el} is the monetary cost of electricity in €/kWh in the case of J_{cost}, and E_{CO2} is the marginal CO_2 emissions of the grid in $kgCO_2$/kWh in the case of J_{CO2}.

$$J_{\Delta u} = \sum_{k=2}^{N} \|u(k) - u(k-1)\|_1 . \tag{6}$$

$$J_\varepsilon = \sum_{k=1}^{N} \varepsilon(k). \tag{7}$$

$$J_{obj} = J_{en} = \sum_{k=1}^{N} \|u(k)\|_1 = \sum_{k=1}^{N} [Q_S(k) + Q_{TES}(k)] . \tag{8}$$

$$J_{obj} = J_{cost} = \sum_{k=1}^{N} \left[P_{el,tot}(k)\right] \cdot \frac{E_{el}(k)}{E_{el,max}}. \tag{9}$$

$$J_{obj} = J_{CO2} = \sum_{k=1}^{N} \left[P_{el,tot}(k)\right] \cdot \frac{E_{CO2}(k)}{E_{CO2,max}}. \tag{10}$$

To obtain a single multi-objective cost function, the three objectives J_ε, $J_{\Delta u}$ and J_{obj} are combined by means of the weighting coefficients α_ε and $\alpha_{\Delta u}$. To adjust the weighting coefficients, Pareto fronts were drawn for every configuration. This process lead to the identification of the coefficients values which best balance the different objectives; these values are presented in TABLE 2.

TABLE 2. Summary of the utilized weighting coefficients.

Mode	HEATING			COOLING		
Objective J_{obj}	J_{en}	J_{cost}	J_{CO2}	J_{en}	J_{cost}	J_{CO2}
Value of α_{ε}	0.8	0.5	0.15	0.6	0.15	0.15
Value of $\alpha_{\Delta u}$	0.05	0.01	0.05	0.05	0.01	0.01
Value of α_{obj}	0.15	0.49	0.8	0.35	0.84	0.84

2) CONSTRAINTS

The constraints on the inputs (i.e. the thermal powers Q_S and Q_{TES}) enable to make the MPC framework aware of the actual limitations of the machine. The binary variables δ_S and δ_{TES} enable to switch the heat pump respectively in space heating/cooling and DHW production mode. As a result, they can never be turned on at the same time, thus $\delta_S(k) + \delta_{TES}(k) \leq 1$. The binary variables also enable to impose a minimum thermal power to be delivered by the heat pump; otherwise the MPC may decide to turn on the heat pump at very low load, which is not representative of the actual behavior of the system. The constraints ranges are: $\left[\underline{Q_{SC}}; \overline{Q}_{SC}\right] = [-8kW; -2.5kW]$ in cooling mode, $\left[\underline{Q_{SH}}; \overline{Q}_{SH}\right] = [3kW; 10kW]$ in heating mode, and $\left[\underline{Q_{TES}}; \overline{Q}_{TES}\right] = [10kW; 10kW]$ in DHW production mode (DHW is always produced at full load).

The constraints on the outputs enable to guarantee a comfort range in the output temperatures T_{int} and T_{TES}. For the inside zone, T_{int} must stay above the boundary $\underline{T_{int}} = 20°$ in winter and below $\overline{T}_{int} = 26°$ in summer to maintain a comfortable indoor environment. For the DHW tank, its temperature T_{TES} must stay above $\underline{T_{TES}} = 50°$ to avoid the growth of legionella. These hard constraints are softened using the slack variable ε: in this way, some small violations of the constraints are allowed, but they are associated with the cost ε in the objective function (see section II.G.1), therefore the MPC will intend to avoid such violations. The constraint relaxation guarantees the feasibility of the OCP even if the initial states are found outside the boundaries (typical at start-up for instance, or due to discrepancy between the model and the actual systems).

H. CONNECTION BETWEEN THE MPC CONTROLLLER AND THE HEAT PUMP

The set-point commands decided by the MPC controller are sent to the heat pump by means of a Modbus gateway available from the manufacturer. Not all the heat pump features can be accessed directly and controlled internally, and several internal protections from the built-in controller cannot be overridden. For instance, even though the frequency of the compressor would be the easiest parameter to control in order to modulate the thermal output as desired, this parameter cannot be accessed directly. Instead, the supply temperature set-points are sent to regulate the heating or cooling thermal power provided by the machine. Four parameters are thus sent to control the heat pump through the gateway: two binary switching variables for activating respectively the space heating/cooling circuit or the DHW circuit, and the two corresponding supply temperature set-points (one for the space conditioning and another one for DHW).

However, the variable optimized by the MPC is the thermal power delivered to the building Q, not the supply temperature set-point T_{sup}, therefore further equations are needed to pass from Q to T_{sup}. These equations are presented in (11) and (12), where $M_S = 0.222\,kW/K$ and $M_{TES} = 2.32\,kW/K$ represent the heat transfer at the level of the FCU and the TES tank, respectively.

$$Q_S = M_S(T_{sup,S} - T_{int}). \tag{11}$$

$$Q_{TES} = M_{TES}(T_{sup,TES} - T_{TES}). \tag{12}$$

TABLE 3. Summary of the investigated scenarios.

Case	Control	Minimization objective	Period
00-Reference	Therm. 21°C	-	HEATING February, 24 to 26th 2018
01-MPC ThEnerg	MPC	Thermal energy	
02-MPC Cost	MPC	Cost	
03-MPC CO_2	MPC	CO_2 marginal emissions	
10-Reference	Therm. 25°C	-	COOLING July, 8th to 10th 2016
11-MPC ThEnerg	MPC	Thermal energy	
12-MPC Cost	MPC	Cost	
13-MPC CO_2	MPC	CO_2 marginal emissions	

I. SUMMARY OF THE SCENARIOS AND BOUNDARY CONDITIONS

TABLE 3 summarizes the scenarios tested in the laboratory. Both in heating and cooling mode, three different MPC configurations are investigated, with the different flexibility objectives. The chosen periods of three days are the 24th to 26th of February 2018 and the 8th to 10th of July 2016: they were selected precisely because they present different weather conditions throughout the three days (cloudy and sunny days) and sufficient variations of the input signals (price and CO_2 emissions). The weather data was retrieved from a weather station located in Tarragona, Spain. The reader is referred to Appendix for more details about the input data used in the different tested cases.

The price data E_{el} used in the MPC Cost configuration corresponds to the PVPC (voluntary price for small consumers), a variable tariff available in Spain for small electricity consumers. The tariff changes every hour, with a sensible step between afternoon and night hours. Furthermore, the hourly prices are public data and thus their forecast can be downloaded directly from the Spanish TSO website [37].

The CO_2 emissions signal E_{CO2} used in the MPC CO_2 configuration actually corresponds to the marginal emissions of the Spanish electrical grid. The marginal emissions provide a more accurate estimation of the CO_2 savings that a flexibility action can generate. They consider the merit order in which the plants are activated to satisfy the demand of

TABLE 4. Energy use, cost and emissions in heating and cooling modes.

Variations compared to the reference case		MPC ThEnerg	MPC Cost	MPC CO_2
		HEATING		
Thermal energy	kWh	+3.23	+12.0	+14.7
	%	+3.78%	+14.0%	+17.2%
Elec. energy	kWh	-3.03	+0.29	-0.88
	%	-8.47%	+0.80%	-2.47%
Cost	€	-0.20	-0.04	+0.21
	%	-5.81%	**-1.03%**	+6.15%
Emissions	$kgCO_2$	-0.90	-0.06	-0.35
	%	-9.16%	-0.60%	-3.59%
Marg. emissions	$kgCO_2$	-0.70	+0.14	-0.32
	%	-7.07%	+1.41%	**-3.29%**
		COOLING		
Thermal energy	kWh	+19.3	+24.3	-11.7
	%	+22.2%	+27.9%	-13.48%
Elec. energy	kWh	+5.01	+5.45	-5.29
	%	+12.8%	+13.9%	-13.5%
Cost	€	+0.50	-0.24	-0.17
	%	+13.9%	**-6.84%**	-4.78%
Emissions	$kgCO_2$	+1.15	+1.38	-1.27
	%	+12.6%	+15.0%	-13.8%
Marg. emissions	$kgCO_2$	+1.19	+1.41	-1.51
	%	+13.0%	+15.4%	**-16.5%**

electricity: for instance, if we reduce our load at a certain moment, the base load (like nuclear) will not be affected by this change, instead the variation will be absorbed by more reactive sources of power (like gas turbines). The marginal emissions factor (MEF) intends to represent such behavior. As a result, the MEF displays variations of higher amplitude than if the average emissions are calculated, and this benefits the MPC configuration by highlighting more clearly the periods of low or high emissions. In the present work, a model of the MEF factor for the Spanish case was used; the calculation methodology is detailed in [38].

III. RESULTS

A. OPERATIONAL COSTS AND EMISSIONS

The MPC strategies implemented aim at enhancing the energy flexibility of the considered building, and more particularly by reducing the operational costs or CO_2 emissions related to the HVAC systems use. These metrics are recounted in III-B, in terms of variations compared to the reference case.

Analyzing the MPC configurations separately enables to analyze their different performance. The MPC ThEnerg scenario operates quite differently in winter and summer: in heating mode, it manages to actually decrease the electricity use by 8.5%, even though the thermal energy (its declared objective) is increased by 3.8%. In cooling mode however, MPC ThEnerg does not perform well and causes significant increases in all the presented quantities: energy, cost and emissions (+12 to 22%). The discrepancy between the two modes might be due to the different value of the weighting coefficient assigned to the comfort sub-objective.

The MPC Cost scenario is able to reduce the operational costs in both seasons, but with a small magnitude. This configuration utilizes the thermal mass of the building and the capacity of the TES tank to store energy during periods of cheaper electricity and restitute it when the price rises again. This storage-like operation causes an increase of the delivered thermal energy because of thermal losses (+14% in heating and +28% in cooling). However since the heat pump is operated more efficiently, the electricity use increases at a lesser rate (+0.8% in heating and +14% in cooling). Furthermore, this electricity use occurs at periods of lower prices, therefore the operational costs are still reduced, by 1.5% in winter and 6.8% in summer. Although this confirms the correct functioning of the MPC Cost strategy, these percentages are rather low for what is expected of economic MPC with such price signals: savings of 7 to 35% are normally reported in the literature [12]. Reasons for this low performance are discussed in the following sections.

A similar analysis can be drawn for the MPC CO_2 configuration in heating mode: despite an increase of the delivered thermal energy (+17%), the marginal CO_2 emissions are reduced, but by a low percentage of 3.3%. In cooling mode, MPC CO_2 manages to yield higher savings, achieving a reduction of 16.5% compared to the reference case. This performance results from a combination of improved energy efficiency (reduction of the thermal energy by 13.5%) and load shifting towards periods where the grid emits less CO_2.

It should be noted that the cost and CO_2 emissions minimization objectives are rather contradictory, as shown in their respective penalty signals in Appendix. Their evolution is symmetric, which means that reducing the cost generally produces an increase of the CO_2 emissions and vice-versa.

B. EFFICIENCY OF THE HEAT PUMP OPERATION

To analyze the efficiency of the heat pump operation, its coefficient of performance (COP) is defined over the whole experiment period of 3 days. It consists of the ratio of the delivered thermal energy by the electrical energy used by the heat pump. The thermal energy comprises both energy for space heating or cooling (in which case the cooling energy is counted as positive) and for DHW production. The electrical energy is integrated over the whole period. It includes the consumption of the outdoor fan, circulating pumps, compressor, and standby power when the machine is not running. These quantities and the calculated COP are represented in Fig. 5.

It can be observed that in general, the MPC operates the heat pump at a higher efficiency, or higher COP, than the reference case. However, the operational COP is lower than the nominal COP declared by the manufacturer, since standby and start-up losses are here included while not in the standard rating conditions. The predictive controller is theoretically

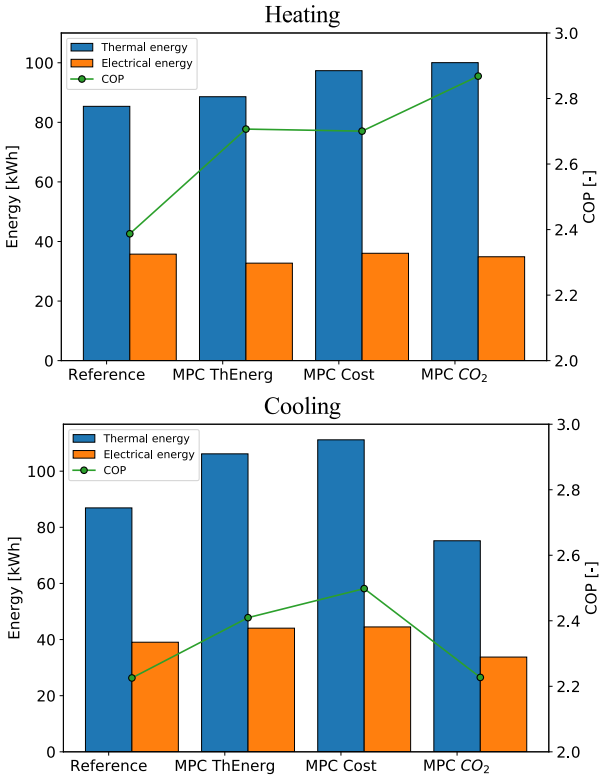

FIGURE 5. Energy and COP analysis in heating and cooling modes.

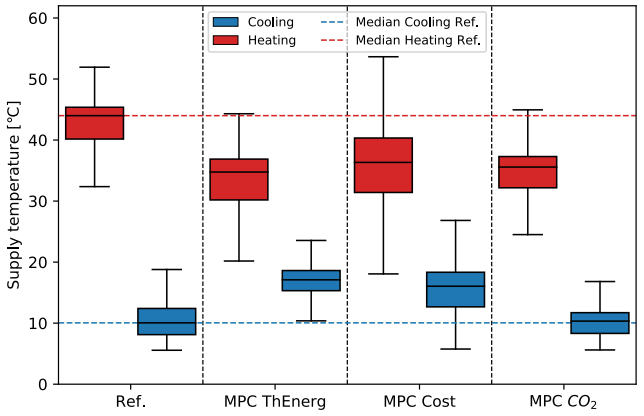

FIGURE 6. Box plots of the supply temperatures in space heating and space cooling modes.

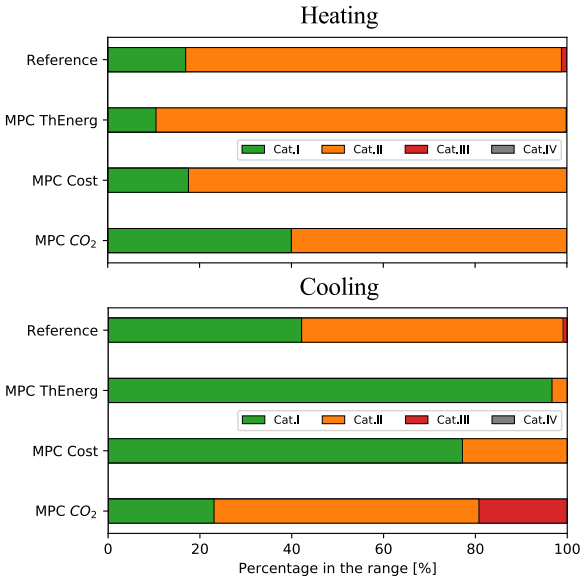

FIGURE 7. Percentage of the time where the indoor operative temperature T_{int} was in the ranges of the comfort categories as defined by the standard [39].

aware of the periods where the efficiency of the heat pump is higher (for instance at milder outdoor temperatures) and thus plans the systems use accordingly. A notable exception is the MPC CO_2 case, which performs quite distinctly in winter and in summer. MPC CO_2 tends to shift the loads towards the afternoon periods, where solar energy is generally available (and hence the grid emissions are lower) and the outdoor temperature is higher. Producing hot water when it is warmer outdoors in winter is much more efficient than when it is colder, which explains the COP gain in the MPC CO_2 in heating mode. In summer, producing cold water at the hottest time of the day brings the efficiency of the heat pump down, therefore the COP falls down at the same level than the reference case.

The differences of efficiency can also partly be explained by the different supply temperatures at which the MPC strategies operate the heat pump. A box plot of the average supply temperatures in space heating and cooling modes is represented in Fig. 6. It can be seen clearly that hot water is produced at lower temperature and cold water at higher temperature than in the reference case, conditions in which the efficiency of the heat pump is improved. MPC CO_2 in cooling mode produces cold water at the same temperature, and thus has the same COP than the reference case.

C. INSPECTION OF THE COMFORT CONDITIONS

Thermal comfort is guaranteed in the MPC framework by the introduction of temperature range constraints on the indoor temperature. These constraints are softened to increase the robustness of the controller, therefore it is important to verify that comfort is not jeopardized during the actual operation of the systems. The comfort analysis is represented in Fig. 7, with the percentages of time where the indoor operative temperature stays within the bounds defined in the standard [39]. These bounds take different values seasonally: Cat.I corresponds to the interval 21-25°C in winter, and 23.5-25.5°C in summer, Cat.II to the interval 20-25°C in winter and 23-26°C in summer.

It can be observed than in heating mode, the comfort level in the MPC cases is similar to the reference case, and thus is maintained at a satisfactory level. The situation is more heterogeneous in cooling mode: MPC ThEnerg operates the building almost all the time in Category I, which is a significant improvement compared to the reference case where only

42% of the time was spent in that category. This explains why this MPC configuration was not capable of saving any energy, cost or emissions. On the other hand, the configuration MPC CO_2 causes a slight decrease of the comfort conditions: incursions in the lower Category III occur during 19% of the time. MPC CO_2 provided the greatest emission savings, but this achievement was reached at the cost of this slight comfort degradation. Category III is still considered as an acceptable comfort range. The difficult trade-off between the comfort of the occupants and the increased flexibility, as reflected in the multi-objective function, is thus perfectly illustrated by these results.

D. LOAD SHIFTING AND FLEXIBILITY

The core of the implemented flexibility control strategies consist in shifting the thermal loads of the building towards periods of lower electricity price or grid CO_2 emissions. To analyze if this shifting effectively occurs and in which proportion, Fig. 8 is plotted: it represents the breakdown of the electricity use of the heat pump according to the low, medium or high penalty periods (price or emissions). Additionally, the consumption is split between the operation modes of the heat pump: space heating (SH) or cooling (SC), DHW and standby mode (SB). In this way, the load shifting can be analyzed in details.

It can be observed that the MPC Cost configuration is the most effective at shifting the loads towards low-penalty periods. In heating mode, the reference case already uses energy mostly in low-price periods, leaving little room for improvement. MPC Cost still manages to improve the shifting of the SH loads: almost no SH operation occurs during high price periods in this case, most of it is displaced in low price hours. The DHW loads are actually shifted in the wrong direction, with an increase of these loads during high price hours. The reasons for this adverse effect will be explained in section IV.IV-A.

In cooling mode, the reference case uses most of the energy in high price periods, therefore MPC Cost has great potential to improve the distribution of the load. It effectively manages to do so and inverse the trend, especially for the SC load which is displaced in great part from high to low price hours. These results reveals the good performance of MPC Cost in cooling mode: by using effectively the available thermal storage of the building (thermal mass and water tank), this control strategy manages to flexibly operate the loads, and thus to relieve the grid at the most critical hours.

The load shifting is much less visible for the MPC CO $_2$ configuration, which shows difficulties in increasing the load at low emission hours. In fact in heating mode, the operation of the systems almost does not differ from the reference case, the energy use at high emissions hours is only slightly reduced, which still provides the benefits aforementioned. In cooling mode, the SC load is almost entirely suppressed of the high emissions periods, but not moved towards the low emissions hours, which results in a lower energy use, greater

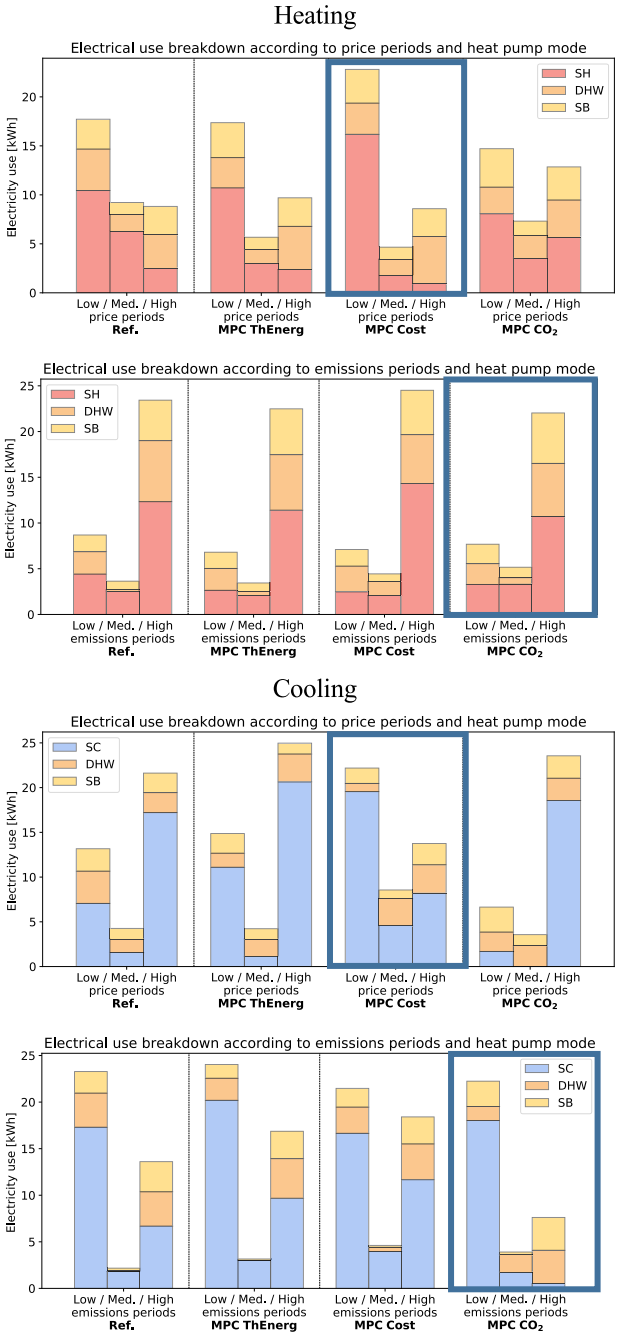

FIGURE 8. Breakdown of the electricity use according to the high/low penalty periods and the heat pump mode (SH/SC, DHW, SB), both in heating and cooling.

emissions savings, at the cost of a slight degradation of the comfort conditions as previously seen in Fig. 7.

IV. DISCUSSIONS ON THE PRACTICAL IMPLEMENTATION OF MPC CONTROLLERS

The analyzed results revealed a positive performance of the implemented MPC strategies, however with a lower effectiveness than expected. Among other reasons, such discrepancies stem from the implementation of the MPC on an actual heat pump, and the bottlenecks that appear when interfacing

the supervisory controller with the physical system, which includes its own local controller. Two of these effects are discussed in the following sections: the DHW tank charging control and the transient effects (ramping especially). Such practical challenges could only be brought up by experimental studies (or alternatively simulation studies with very detailed transient models), and they are therefore considered as valuable learnings and part of the work output.

A. DHW TANK CHARGING

It was shown in the flexibility analysis that the MPC strategies often failed to shift the DHW load to the low penalty periods (whether price or emissions), and even sometimes shifted this load to high penalty periods. This adverse effect can partly be explained by the interfacing between the supervisory and the local controller of the heat pump. The command to activate the DHW tank charging through the Modbus gateway is called ''Control DHW Run/Stop'' in the manufacturer manual. Sending a 0 to this input effectively prevents the DHW operation of the heat pump. However, sending a 1 does not automatically provoke the tank charging: it only corresponds to an ''availability'' of the DHW operation, the built-in controller then determines if it needs to be activated, based on the temperature in the tank. The local controller considers the actual set-point and a negative deadband of 5°C which can be set in the local controller (5°C is the minimum): for instance, if the set-point is 55°C and the water in the tank is 51°C when the activation signal for DHW is sent, the heat pump will not start. This is problematic if the MPC intends to precharge the tank at some times where the local controller would not deem it necessary. The principle of MPC to utilize the TES by overheating it in some favorable periods and discharging it at others periods is thus hindered by the interaction with the local controller. This problem does not occur in the other circuit of the heat pump which supplies SH/SC: the equivalent command is called ''Control Circuit 1 Run/Stop'', and sending a 1 to this input always results in an activation of the heat pump.

An example of the DHW charging bottleneck is illustrated in Fig. 8. On the top graph, the SC binary command is represented, on the second graph the DHW binary command, on the third graph the response of the heat pump in terms of its compressor frequency, and in the bottom graph the tank temperature. One can observe that the first 5 activation requests (4 of SC, 1 of DHW) are correctly followed by an activation of the heat pump compressor. The 6^{th} requested activation (DHW) does not result in an actual operation of the heat pump: the water temperature at that moment was 50°C, therefore not sufficiently low for the built-in controller to order the DHW tank charging. As a result, the MPC must reschedule the tank charging at the subsequent iterations, and two later DHW activations are thus observed. This can pose a problem to the performance of the MPC: if the tank charging was initially planned at a low-penalty period, the reschedule could occur at less favorable periods in terms of price or CO_2 emissions. This partly explains the poor performance of the DHW load shifting and the fact that it is sometimes shifted to high penalty periods.

On average, the charging of the DHW tank occurred 17 times over the studied periods of 3 days. A DHW command was sent on average 12 additional times and ignored by the local controller of the heat pump. This situation thus occurred quite frequently, which explains why the MPC struggled to shift the DHW loads. This offers as valuable learning that the implementation of an MPC controller with a real heat pump is not a straightforward process. Oftentimes, the functioning of the local controllers built in the machine are not described clearly by the manufacturer, and the developer must therefore consider the heat pump as a black box and realize tests to observe its behavior in-situ. This increases the development costs of the controller and its implementation, while they are already high due to the required modelling (60% of the costs mentioned in [36]).

Potential solutions to overcome the DHW charging limitation include:

- Instead of using the set-point determined by the MPC solution, always set it to the maximum (60°C for instance). The modulation potential of the MPC would be lost, and the tank might be overheated for its actual use, but the DHW charging should occur with more probability.
- The deadband could also be reduced. In the present case, the minimum is 5°C so it is not possible, but other heat pump models might let the installer set smaller values. Such protection enables to avoid too many switching of the DHW charging mode, but this can be managed in other ways by an MPC controller.
- Another possibility would be to choose a heat pump where an explicit control of the DHW charging is possible, or to use other inputs (such as the booster or the anti-legionella setting, but these are made for other purposes and generally use the electrical resistance to provide fast heating at high temperatures).

B. TRANSIENT AND DYNAMIC EFFECTS

The transitory phases constitute another aspect proper to the dynamics of a real heat pump operation. The MPC controller computes an optimal plan considering that the heat pump will effectively deliver heat at the correct set-point, with the desired constant thermal power. However, many dynamic effects occur in reality which make the actual operation differ from the MPC scheduled plan.

To illustrate this point, Fig. 9 is plotted. On the top graph, the plan of the MPC is shown: the controller scheduled to operate space heating during 48 minutes, at a thermal power of around 6 kW. The measured thermal power (calculated with the temperature lift and the mass flow rate) is also represented, and a clear discrepancy can already be observed. On the second graph, the supply and return temperatures are plotted, on the third graph the frequency of the heat pump compressor and on the bottom graph, the zone temperature in

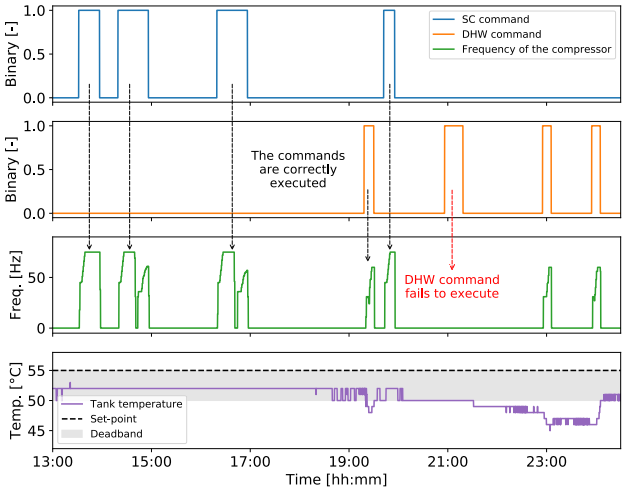

FIGURE 9. Example of non-execution of the DHW production command.

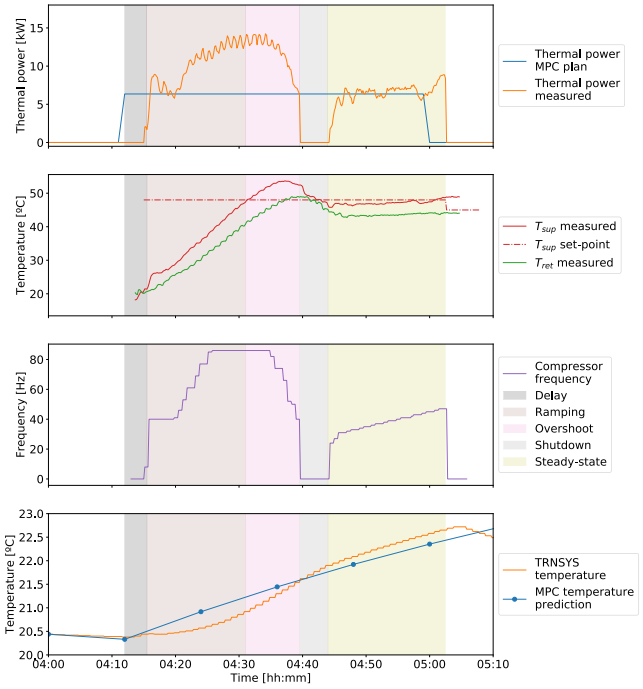

FIGURE 10. Example of an activation of space heating, where the delay and the ramping effects can clearly be observed.

the building (both predicted by the MPC and as happened in the actual simulation) is represented.

In this example, the operation of the space heating activation is separated in 5 phases highlighted by different background colors. The last phase is the quasi steady-state during which the heat pump operate according to plan: the measured and planned thermal powers coincide, and the heat pump supplies water at a temperature close to the desired set-point of 48°C. This operation confirms that the heat pump performance has been represented correctly, since its model was based on points measured in steady-state too. However, before to reach this steady-state operation, the systems go through other successive phases, which are not anticipated by the MPC.

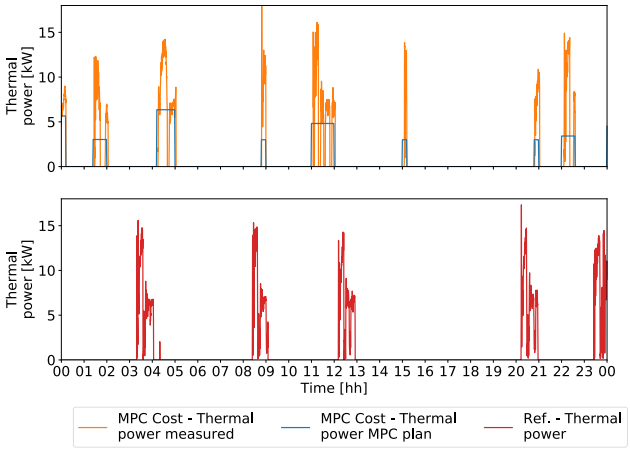

FIGURE 11. Comparison over one day between the reference case and one MPC case (MPC cost).

Firstly, a delay is observed before the heat pump reacts, and the compressor only starts few minutes after the commands are sent. Secondly, after the compressor has started running, a ramping phase occurs: the heat pump starts with a plateau due to its internal control, and then increases its power gradually. Since the water had cooled down since the last activation, the system starts a lower temperature and must ramp progressively to achieve the desired set-point. However, this increase is slow and takes at least 15 minutes in the present case. Contrary to a boiler, the temperature lift of a heat pump is rather limited (around 5°C normally), and thus the system must "wait" for the return temperature to also increase so that the supply temperature can reach the desired value. At the end of the ramping phase, the compressor frequency has reached a maximum and therefore the actual thermal power is significantly higher than anticipated by the MPC. This observation partly explains why the delivered thermal energy is increased in most MPC cases. During the third phase, an overshoot effect occurs: the supply temperature overcomes the desired set-point and thus the heat pump starts to decrease the compressor frequency. However, due to the inertia of the systems and the delayed internal control of the machine, the supply temperature still reaches the value of a protection deadband (+5°C above the set-point), causing a shutdown of the compressor, which is the fourth phase. The shutdown lasts around 5 minutes, and then the compressor is switched on again and starts the steady-state phase.

The transient phases partly explain why the MPC strategies have a relatively limited performance. For instance, if the space heating activations are short, the heat pump stays in the transient phases and do not reach the steady state, therefore its delivered power is higher than anticipated and this causes the final increase in thermal energy observed in most cases. The fluctuations in power could also cause trouble for direct control schemes of demand response with heat pumps: if an aggregator or utility requires a certain level of power from the heat pump load during a fixed period, they must be aware that this power might be delayed

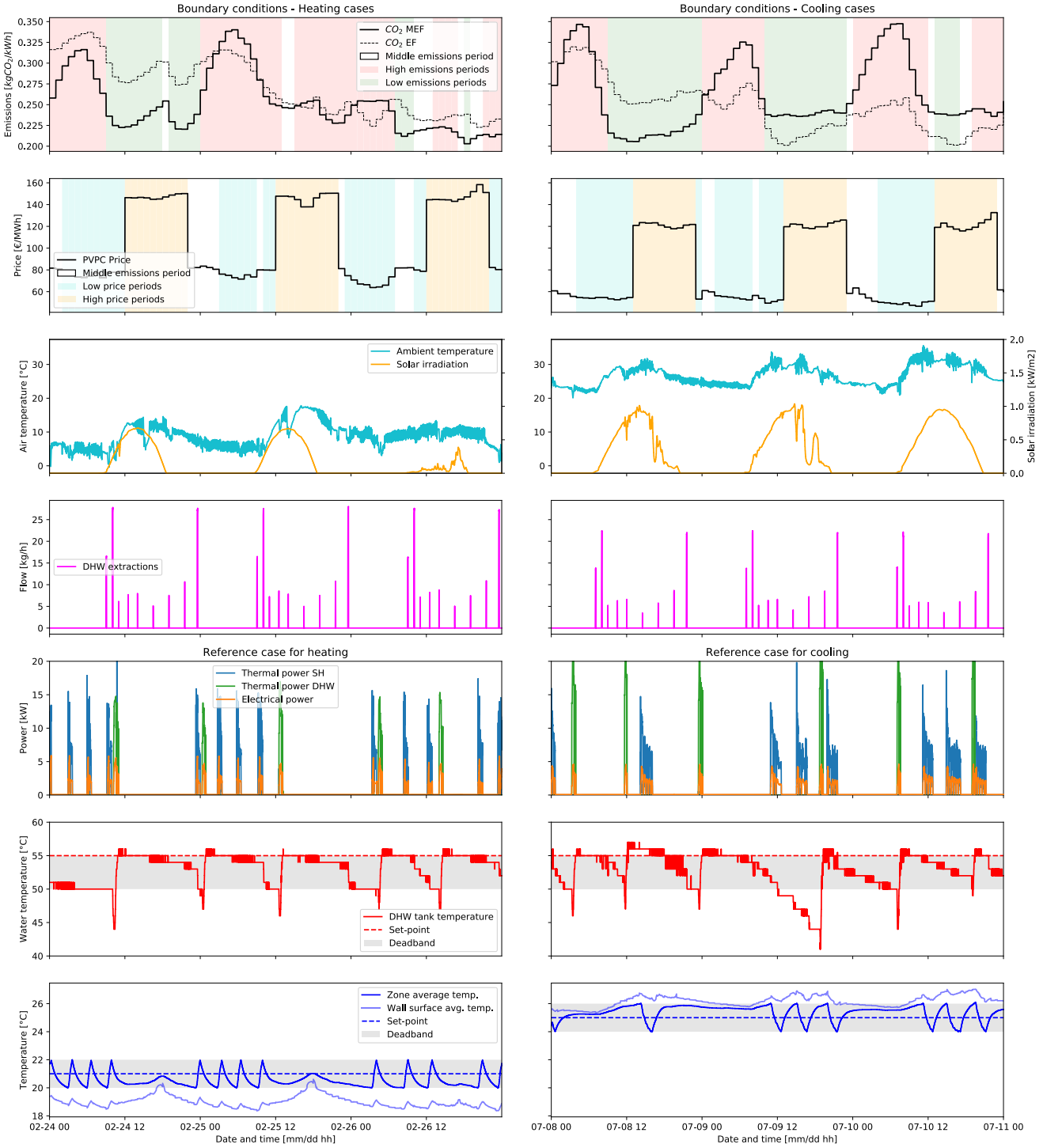

FIGURE 12. Boundary conditions and reference cases.

or not guaranteed during the whole period (shutdown or cycling).

These transient phases only explain partly the performance, other phenomena can play a role in the observed effects. Notably, the heat pump operates at milder temperatures as demonstrated in Fig. 6 and this displacement of the operating point to another region of the performance map can also cause an increase of the thermal power with respect to the reference case. The inability of the compressor to modulate its output below 30 Hz additionally participates in increasing the on-off cycling and to generate discrepancies compared to the desired MPC plan.

To quantify the actual effect of the thermal power overshoot on the overall dynamic behavior, Fig. 11 is plotted.

It represents the thermal powers (planned by the MPC and measured) in the MPC Cost case over 24 hours, compared to the reference case. The increase of thermal energy compared to the MPC plan is clearly visible: the MPC solution required to deliver only 16.7 kWh during this day, while 24.4 kWh were actually supplied to the building, which represents an increase of 45%. Furthermore, in this case space heating is activated 4 times in the reference case, and 8 times in the MPC case: doubling the number of cycles results in a higher impact of the overshooting effect on the overall performance.

The overshoot and transient phases also occur in the reference case, however since the thermostat controller do not work in a predictive manner, this mismatch does not affect it as much as in the MPC cases. For that case, the thermostat shuts down the heating when the delivered energy equals what is needed to reach the desired set-point, thus if the heat pump delivers more heat, the thermostat will stop before. On the other hand, a predictive controller makes a plan beforehand and expects it to be complied with, therefore the unexpected transient effects have a greater influence on it.

The main issue regarding the start-up phase is that it is difficult to model within the MPC framework. The model is correct in steady-state as previously mentioned, only a correction is needed to account for the successive transient phases when the heat pump is switched on. Potential solutions include:

- Applying a constant coefficient to consider the excess thermal power of the start-up transitory phases. This coefficient should reflect the ratio between the delivered energy during a total activation period and the planned energy (integrals of the two curves on the top graph of Fig. 11). In this way, the set-point sent to the heat pump will be slightly lower, and the delivered thermal energy should match better with the MPC plan.
- Increasing the discretization time step of the MPC (now set to 12 min) might also improve the performance: in this way, the heat pump will stay activated during longer periods and thus the start-up phase will have a lesser importance overall.
- The relative importance of the smoothing term in the multi-objective function could also be increased. This would provoke the heat pump to operate for longer periods since too many switching will be highly penalized. The steady-state will thus last longer and take a larger proportion compared to the transient phases, reducing the influence of the latter.

V. CONCLUSIONS

Different configurations of MPC for heat pumps were investigated experimentally, all of them leveraging the existing thermal storage of a residential building, which consist for one part of its inherent thermal mass and for the other part of a DHW tank. Operating these two types of TES in a flexible manner, the MPC could yield a significant shifting of the thermal building loads towards periods of cheaper electricity or lesser carbon intensity of the grid. As a result, the MPC strategy aiming to minimize the operational costs of the heat pump managed to reduce them by 1 to 7% and the one minimizing the marginal CO_2 emissions managed to reduce them by 3 to 17%, despite an increase of the actual energy use in most cases. This confirms the potential of predictive controllers, however the savings did not reach the expected magnitude observed in most simulation works published so far in the literature.

The efficiency of the systems was improved by the MPC configurations, which make use of the knowledge about the performance of the heat pump depending on the operating conditions. The MPC thus operate the heat pump at milder supply temperature in all MPC cases except one, which benefits the overall COP. Thermal comfort of the occupants is generally maintained in the analyzed scenarios in winter and summer, although some fluctuations occur, especially in cooling mode.

The development process of the MPC revealed the difficult task of finding a trade-off between the different aspects of building energy flexibility, so that it benefits all involved parties (utilities, end-users and society as a whole). In general, the MPC strategies manage to find a balance between the sometimes contradictory objectives (cost, comfort, carbon footprint, flexibility etc.), although they sometimes emphasize one aspect at the cost of another one. The fine-tuning of the weighting coefficients in the multi-objective cost function plays an important role in finding a satisfactory tradeoff.

Additionally, the experimental nature of the study enabled to highlight the practical bottlenecks that arose from the implementation on a real heat pump system. In particular, the interaction with the local controller of the heat pump and the transient phases that are not modelled by the MPC have been discussed and still constitute some practical challenges to the implementation of such controllers at a large scale. Solutions to these identified barriers are proposed. Further work includes the testing of these proposals, the comparison with simpler rule-based controls and the investigation of the control strategies with different building typologies.

Finally, the results highlighted the promising potential of utilizing the existing thermal energy storages present in residential buildings both in summer and winter modes. These means of storage are readily available and do not require further equipment investment to be exploited for energy flexibility purposes. Only adapted control strategies like the MPC controllers presented in this work need to be developed to leverage their full potential and store energy at the most beneficial times to restore it subsequently. Managing and aggregating the capacity of individual buildings equipped with heat pumps into a larger scale storage system also constitutes a promising topic for further research.

APPENDIX
BOUNDARY CONDITIONS AND REFERENCE CASES

See Fig. 12.

ACKNOWLEDGMENT

Part of this work contributes to the activities carried out in the framework of the IEA-EBC Annex 67 (International Energy Agency – Energy in Buildings and Communities program) about Energy Flexibility in Buildings.

The authors would like to acknowledge the work of Ivan Bellanco and Juan Francisco Belio Gil from the SEILAB laboratory in Tarragona (Spain), who actively participated in the physical setup of the laboratory and the development of the digital interface necessary for the experimental part of this work.

REFERENCES

[1] *Special Report on Global Warming of 1.5oC*, Intergovernmental Panel on Climate Change (IPCC), Incheon, Republic of Korea, 2018.
[2] B. Kroposki *et al.*, "Achieving a 100% renewable grid: Operating electric power systems with extremely high levels of variable renewable energy," *IEEE Power Energy Mag.*, vol. 15, no. 2, pp. 61–73, Mar./Apr. 2017.
[3] *Renewable Energy Policies in a Time of Transition*, IRENA, IEA, and REN21, Abu Dhabi, UAE, 2018.
[4] R. H. Byrne, T. A. Nguyen, D. A. Copp, B. R. Chalamala, and I. Gyuk, "Energy management and optimization methods for grid energy storage systems," *IEEE Access*, vol. 6, pp. 13231–13260, 2017.
[5] A. Arteconi, N. J. Hewitt, and F. Polonara, "State of the art of thermal storage for demand-side management," *Appl. Energy*, vol. 93, pp. 371–389, May 2012.
[6] J. Heier, C. Bales, and V. Martin, "Combining thermal energy storage with buildings—A review," *Renew. Sustain. Energy Rev.*, vol. 42, pp. 1305–1325, Feb. 2015.
[7] G. Reynders, J. Diriken, and D. Saelens, "Generic characterization method for energy flexibility: Applied to structural thermal storage in residential buildings," *Appl. Energy*, vol. 198, pp. 192–202, Jul. 2017.
[8] S. Ø. Jensen *et al.*, "IEA EBC annex 67 energy flexible buildings," *Energy Build.*, vol. 155, pp. 25–34, Aug. 2017.
[9] D. I. Mendoza-Serrano and D. J. Chmielewski, "Controller and system design for HVAC with thermal energy storage," in *Proc. Amer. Control Conf.*, 2012, pp. 3669–3674.
[10] K. Amarasinghe, D. Wijayasekara, H. Carey, M. Manic, D. He, and W.-P. Chen, "Artificial neural networks based thermal energy storage control for buildings," in *Proc. IECON 41st Annu. Conf. IEEE Ind. Electron. Soc.*, Nov. 2015, pp. 5421–5426.
[11] B. Venkatesh, "Thermal energy storage for homes," in *Proc. IEEE Int. Conf. Smart Energy Grid Eng.*, Aug. 2018, pp. 36–39.
[12] D. Fischer and H. Madani, "On heat pumps in smart grids: A review," *Renew. Sustain. Energy Rev.*, vol. 70, pp. 342–357, Oct. 2017.
[13] T. Q. Péan, J. Salom, and R. Costa-Castelló, "Review of control strategies for improving the energy flexibility provided by heat pump systems in buildings," *J. Process Control*, vol. 74C, pp. 35–49, Apr. 2019.
[14] G. Papaefthymiou, B. Hasche, and C. Nabe, "Potential of heat pumps for demand side management and wind power integration in the German electricity market," *IEEE Trans. Sustain. Energy*, vol. 3, no. 4, pp. 636–642, Oct. 2012.
[15] B. Biegel, P. Andersen, T. S. Pedersen, K. M. Nielsen, J. Stoustrup, and L. H. Hansen, "Electricity market optimization of heat pump portfolio," in *Proc. IEEE Int. Conf. Control Appl.*, Aug. 2013, pp. 294–301.
[16] G. Masy, E. Georges, C. Verhelst, and V. Lemort, "Smart grid energy flexible buildings through the use of heat pumps and building thermal mass as energy storage in the Belgian context," *Sci. Technol. Built Environ.*, vol. 21, pp. 800–811, Aug. 2015.
[17] R. Halvgaard, N. K. Poulsen, H. Madsen, and J. B. Jorgensen, "Economic model predictive control for building climate control in a smart grid," in *Proc. IEEE PES Innov. Smart Grid Technol.*, Jan. 2012, pp. 1–6.
[18] R. De Coninck and L. Helsen, "Practical implementation and evaluation of model predictive control for an office building in Brussels," *Energy Build.*, vol. 111, pp. 290–298, Jan. 2016.
[19] D. Fischer, T. Wolf, and M.-A. Triebel, "Flexibility of heat pump pools: The use of SG-ready from an aggregator's perspective," in *Proc. 12th IEA Heat Pump Conf.*, 2017, pp. 1–12.
[20] D. Xie, L. Yu, T. Jiang, and Y. Zou, "Distributed energy optimization for HVAC systems in University campus buildings," *IEEE Access*, vol. 6, pp. 59141–59151, 2018.
[21] T. Jiang and G. Deng, "Optimizing the low-carbon flexible job shop scheduling problem considering energy consumption," *IEEE Access*, vol. 6, pp. 46346–46355, 2018.
[22] G. Lowry, "Day-ahead forecasting of grid carbon intensity in support of heating, ventilation and air-conditioning plant demand response decision-making to reduce carbon emissions," *Build. Serv. Eng. Res. Technol.*, vol. 39, no. 6, pp. 749–760, 2018.
[23] P. J. C. Vogler-Finck, R. Wisniewski, and P. Popovski, "Reducing the carbon footprint of house heating through model predictive control—A simulation study in Danish conditions," *Sustain. Cities Soc.*, vol. 42, pp. 558–573, Jan. 2018.
[24] J. Clauß, S. Stinner, I. Sartori, and L. Georges, "Predictive rule-based control to activate the energy flexibility of Norwegian residential buildings: Case of an air-source heat pump and direct electric heating," *Appl. Energy*, vol. 237, pp. 500–518, Mar. 2019.
[25] T. Q. Péan, J. Salom, and J. Ortiz, "Environmental and economic impact of demand response strategies for energy flexible buildings," *Build. Simul. Optim. BSO*, Sep. 2018, pp. 11–12.
[26] L. A. Hurtado, J. D. Rhodes, P. H. Nguyen, I. G. Kamphuis, and M. E. Webber, "Quantifying demand flexibility based on structural thermal storage and comfort management of non-residential buildings: A comparison between hot and cold climate zones," *Appl. Energy*, vol. 195, pp. 1047–1054, Jun. 2017.
[27] K.-H. Lee, M.-C. Joo, and N.-C. Baek, "Experimental evaluation of simple thermal storage control strategies in low-energy solar houses to reduce electricity consumption during grid on-peak periods," *Energies*, vol. 8, no. 9, pp. 9344–9364, 2015.
[28] S. A. Klein, W. A. Beckman, J. W. Mitchel, J. A. Duffie, N. A. Duffie, and T. L. Freeman, *TRNSYS Manual*. Madison, WI, USA: Univ. Wisconsin-Madison, 2009.
[29] N. Alibabaei, A. S. Fung, and K. Raahemifar, "Development of MATLAB-TRNSYS co-simulator for applying predictive strategy planning models on residential house HVAC system," *Energy Build.*, vol. 128, pp. 81–98, Sep. 2016.
[30] T. Q. Péan and J. Salom, "Laboratory facilities used to test energy flexibility in buildings—A technical report from IEA EBC annex 67 energy flexible buildings," IEA EBC Annex, Taastrup, Denmark, Tech. Rep., 2017.
[31] *EN 12976-2—Thermal Solar Systems and Components—Factory Made Systems—Part 2: Test Methods*, CEN, Brussels, Belgium, 2017.
[32] *EU Buildings Database*. European Commission—Energy, 2018. Accessed: Dec. 5, 2018. [Online]. Available: https://ec.europa.eu/energy/en/eu-buildings-database
[33] J. Ortiz, F. Guarino, J. Salom, C. Corchero, and M. Cellura, "Stochastic model for electrical loads in Mediterranean residential buildings: Validation and applications," *Energy Build.*, vol. 80, pp. 23–36, Sep. 2014.
[34] G. Reynders, J. Diriken, and D. Saelens, "Quality of grey-box models and identified parameters as function of the accuracy of input and observation signals," *Energy Build.*, vol. 82, pp. 263–274, Oct. 2014.
[35] P. Bacher and H. Madsen, "Identifying suitable models for the heat dynamics of buildings," *Energy Build.*, vol. 43, no. 7, pp. 1511–1522, 2011.
[36] H. Thieblemont, F. Haghighat, R. Ooka, and A. Moreau, "Predictive control strategies based on weather forecast in buildings with energy storage system: A review of the state-of-the art," *Energy Build.*, vol. 153, pp. 485–500, Oct. 2017.
[37] Red Electrica de España. *ESIOS—Sistema de información del operador del sistema*. Accessed: Jul. 3, 2018. [Online]. Available: https://www.esios.ree.es/en
[38] T. Q. Péan, J. Salom, and J. Ortiz, "Environmental and economic impact of demand response strategies for energy flexible buildings," in *Proc. Building Simul. Optim. (BSO)*, Cambridge, U.K., Sep. 2018, pp. 277–283.
[39] *Indoor Environmental Input Parameters for Design and Assessment of energy performance of Buildings Addressing Indoor Quality, Thermal Environment, Lighting and Acoustic*, Standard EN 15251, CEN, European Committee for Standardization, Brussels, Belgium, 2007.
[40] *Air Conditioners, Liquid Chilling Packages and Heat Pumps With Electrically Driven Compressors for Space Heating and Cooling—Part 2: Test Conditions*, Standard EN 14511-2, CEN, Brussels, Belgium, 2012.

THIBAULT PÉAN was born in Angers, France, in 1990. He received the M.Sc. degree in general engineering from the École Centrale de Nantes, France, in 2012, and the M.Sc. degree in architectural engineering from the Technical University of Denmark (DTU), in 2014. He is currently pursuing the Ph.D. degree with the Polytechnic University of Catalonia.

From 2015 to 2016, he was a Research Assistant with the International Centre for Indoor Environment and Energy, DTU. Since 2016, he has been a Researcher with the Institut de Recerca en Energia de Catalunya. He received the Marie Sklodowska-Curie Actions Scholarship to carry out his Ph.D. in automatic control, which specializes in the control of heat pumps for providing energy flexibility in buildings. He is also a Student Member of ASHRAE.

RAMON COSTA-CASTELLÓ (SM'97) was born in Lleida, Spain, in 1970. He received the B.S. degree in computer science from the Universitat Politècnica de Catalunya (UPC), in 1993, and the Ph.D. degree in computer science from the Advanced Automation and Robotics Program, UPC, in 2001, where he is currently an Associate Professor with the Automatic Control Department. He is also currently with the Institut de Robòtica i Informàtica Industrial (CSIC-UPC), Barcelona, Spain His teaching activity is related to different aspects of automatic control. His research interests include the analysis and development of energy management (automotive and stationary applications) and the development of digital control techniques. He is a member of CEA and IFAC (EDCOM, TC 9.4 Committee, and Automotive Control TC 7.1.

ELENA FUENTES received the Ph.D. degree from the Polytechnic University of Valencia, Valencia, Spain, in 2006. She was a Research Associate with The University of Manchester, Manchester, U.K., from 2006 to 2012. She is currently the Head of the Laboratory, Institut de Recerca en Energia de Catalunya, Barcelona, Spain, which includes semi-virtual facilities for the analysis of the performance and integration of energy systems. Her current research interests include the experimental characterization of the energy efficiency of HVAC equipment and their optimal integration in distributed energy systems, together with the adaptation to demand-side response, and flexibility in buildings.

JAUME SALOM received the Ph.D. degree in thermal engineering. He is a Lead Researcher and is currently the Group Leader of the Thermal Energy and Building Performance Group (ETE) and Energy Efficiency Systems, Building and Communities (ECOS), IREC. He has a relevant experience leading and participating in international and national research and development projects in the field of building physics, and the simulation of energy systems. Since the creation of its research group, IREC, in 2010, relevant work has been done in the field of energy efficiency in buildings, the concept of net zero energy buildings and load match and grid interaction and the development of advanced concepts, and tools for renewable energy supply of IT data centers.